AMERICAN SOCIETY FOR MICROBIOLOGY | mSphere®

RESEARCH ARTICLE

Andes Virus Genome Mutations That Are Likely Associated with Animal Model Attenuation and Human Person-to-Person Transmission

Carla M. Bellomo,[a] Daniel O. Alonso,[a] Unai Pérez-Sautu,[b] Karla Prieto,[b,c] Sebastian Kehl,[a] Rocio M. Coelho,[a] Natalia Periolo,[a] Nicholas Di Paola,[b] Natalia Ferressini-Gerpe,[d] Jens H. Kuhn,[e] Mariano Sanchez-Lockhart,[b] Gustavo Palacios,[d,f] Valeria P. Martínez[a]

[a]Laboratorio Nacional de Referencia de Hantavirus, Instituto Nacional de Enfermedades Infecciosas, Administración Nacional de Laboratorios e Institutos de Salud Dr. Carlos G. Malbran, Buenos Aires, Argentina

[b]Center for Genome Sciences, United States Army Medical Research Institute of Infectious Diseases, Fort Detrick, Frederick, Maryland, USA

[c]College of Public Health, University of Nebraska Medical Center, Omaha, Nebraska, USA

[d]Department of Microbiology, Icahn School of Medicine at Mount Sinai, New York, New York, USA

[e]Integrated Research Facility at Fort Detrick, Division of Clinical Research, National Institute of Allergy and Infectious Diseases, National Institutes of Health, Fort Detrick, Frederick, Maryland, USA

[f]Global Health Emerging Pathogen Institute, Icahn School of Medicine at Mount Sinai, New York, New York, USA

Carla M. Bellomo, Daniel O. Alonso, Gustavo Palacios, and Valeria P. Martínez contributed equally to the study. Author order was determined by decreasing seniority level.

ABSTRACT We performed whole-genome sequencing with bait enrichment techniques to analyze Andes virus (ANDV), a cause of human hantavirus pulmonary syndrome. We used cryopreserved lung tissues from a naturally infected long-tailed colilargo, including early, intermediate, and late cell culture, passages of an ANDV isolate from that animal, and lung tissues from golden hamsters experimentally exposed to that ANDV isolate. The resulting complete genome sequences were subjected to detailed comparative genomic analysis against American orthohantaviruses. We identified four amino acid substitutions related to cell culture adaptation that resulted in attenuation of ANDV in the typically lethal golden hamster animal model of hantavirus pulmonary syndrome. Changes in the ANDV nucleocapsid protein, glycoprotein, and small nonstructural protein open reading frames correlated with mutations typical for ANDV strains associated with increased virulence in the small-animal model. Finally, we identified three amino acid substitutions, two in the small nonstructural protein and one in the glycoprotein, that were only present in the clade of viruses associated with efficient person-to-person transmission. Our results indicate that there are single-nucleotide polymorphisms that could be used to predict strain-specific ANDV virulence and/or transmissibility.

IMPORTANCE Several orthohantaviruses cause the zoonotic disease hantavirus pulmonary syndrome (HPS) in the Americas. Among them, HPS caused by Andes virus (ANDV) is of great public health concern because it is associated with the highest case fatality rate (up to 50%). ANDV is also the only orthohantavirus associated with relatively robust evidence of person-to-person transmission. This work reveals nucleotide changes in the ANDV genome that are associated with virulence attenuation in an animal model and increased transmissibility in humans. These findings may pave the way to early severity predictions in future ANDV-caused HPS outbreaks.

KEYWORDS comparative genomics, orthohantavirus, person-to-person transmission

Approximately 25 rodent-borne orthohantaviruses (order *Bunyavirales*, family *Hantaviridae*, genus *Orthohantavirus*) have been identified as etiologic agents of human hantavirus pulmonary syndrome (HPS) in the Americas (1). In Argentina, most HPS cases are caused by

Editor Martin Schwemmle, University Medical Center Freiburg

This is a work of the U.S. Government and is not subject to copyright protection in the United States. Foreign copyrights may apply.

Address correspondence to Gustavo Palacios, Gustavo.palacios@mssm.edu, or Valeria P. Martínez, valepm@gmail.com.

The authors declare no conflict of interest.

Received 17 January 2023
Accepted 24 March 2023

Downloaded from https://journals.asm.org/journal/msphere on 06 June 2023 by 200.51.93.114.

Andes virus (ANDV) and somewhat uncharacterized ANDV-like viruses (e.g., Buenos Aires virus [BASV], Lechiguanas virus [LECV], and Orán virus [ORNV]). HPS has a case fatality range of 21 to 50%, with ANDV typically causing the highest lethality (2–5). American orthohantaviruses are pathogenic for humans and subclinically infect cricetid rodents in nature; ANDV is primarily maintained by long-tailed colilargos (*Oligoryzomys longicaudatus* (Bennett, 1832)) (6).

The route of orthohantavirus transmission to humans is typically zoonotic, i.e., from rodents to humans via contaminated rodent secreta or excreta in the absence of intermediate nonmammalian vectors (7). However, in 1996, an HPS outbreak caused by ANDV strain Epilink/96 that began in El Bolsón, Río Negro Province, Argentina, was attributed for the first time to person-to-person transmission (4, 8, 9). Sporadic HPS outbreaks with very limited person-to-person ANDV transmission have occurred over the last 25 years (2, 3, 10). Recently, state-of-the-art molecular epidemiology applied to a 2018–2019 HPS outbreak in Epuyén, Chubut Province, Argentina, confirmed the unique capacity of some strains of ANDV (in this instance, ANDV/Epuyén/18-19) to sustain forward orthohantavirus transmission in humans (11).

ANDV and Maporal virus (MAPV) are the only orthohantaviruses that have been documented to reproduce key features of HPS and cause lethal disease in a rodent model, i.e., golden hamsters [*Mesocricetus auratus* (Waterhouse, 1839)] (12–14). Immunocompetent golden hamsters provide uniformly lethal results when exposed to the Chilean strain ANDV/CHI-9717869 (isolated from a long-tailed colilargo collected from Lago Atravesado, Coyhaique, Aysen Region, Chile, in 1997) (12, 15) or the Argentinean strain ANDV/ARG (isolated from a long-tailed colilargo collected in the vicinity of the primordial site of discovery of ANDV [El Bolsón] in 2000) (14). However, the golden hamster model did not produce lethal results when exposed to a closely related strain, ANDV/CHI-7913 (isolated from clinical samples from a fatal case that was a family contact of the index case of an outbreak near Santiago, Chile, in 1999) (16, 17). These findings indicated that subtle strain-specific genomic differences may have dramatic phenotypic consequences (17).

Cell culture passaging has been associated with viral virulence attenuation for multiple orthohantaviruses in animal models (18, 19). We therefore hypothesized that serial cell culture passaging of an ANDV known to be uniformly lethal in golden hamsters would result in attenuation, that attenuation would be traceable to specific mutations in the ANDV genome, and that these mutations may be catalysts for ANDV adaptation and therefore possible predictive markers for virulence and/or transmissibility.

RESULTS

Cell culture passaging of Andes virus strain ARG results in virulence attenuation *in vivo*. Andes virus strain ARG (ANDV/ARG) is one of a select few available strains isolated directly from the rodent reservoir, long-tailed colilargos (20). To our knowledge, it is also the only ANDV strain directly sequenced from rodent material (passage 0 [p0]). We hypothesized that cell culture passaging attenuates ANDV/ARG. To test this hypothesis, we passaged ANDV/ARG p9, described previously as causing 100% lethality in golden hamsters at 10 days after exposure (14), an additional 10 times in grivet Vero E6 cells (to p19). In a side-by-side comparison, all golden hamsters exposed via intramuscular injection of ANDV/ARG p9 uniformly reached euthanasia criteria, as expected, whereas 33.3% of those exposed to ANDV/ARG p19 recovered, and mock-exposed control animals uniformly survived (Fig. 1). Kaplan-Meier comparison of survival curves and log rank tests (Mantel-Cox [$P < 0.0001$; chi-square = 18.47], trend variation with the number of passages [$P = 0.0101$; chi-square = 6.610], and Gehan-Breslow-Wilcoxon [$P = 0.0005$; chi-square = 15.13]) demonstrated that these survival differences are statistically significant. ANDV/ARG RNA was consistently detected in golden hamster lung samples (3.8×10^6 to 1.7×10^{10} RNA copies per 100 mg of perfused tissue) in the ANDV/ARG p9 and p19 cohorts but not in the mock-exposed control cohort.

Phylogenetic analysis informs the evolutionary history of Buenos Aires virus and Andes virus strain ARG. We performed phylogenetic analysis of ANDV/ARG and Buenos Aires virus (BASV) small (S) and medium (M) genomic segments as well as the

Downloaded from https://journals.asm.org/journal/msphere on 06 June 2023 by 200.51.93.114.

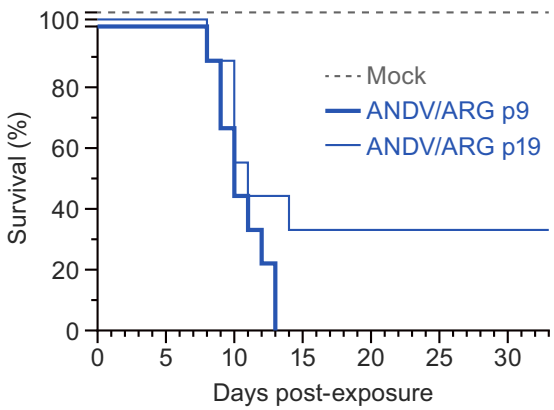

FIG 1 Cell culture passaging of Andes virus results in virulence attenuation *in vivo*. Shown are Kaplan-Meier survival curves of golden hamsters inoculated intramuscularly with three different preparations until the study endpoint. ANDV/ARG, Andes virus strain ARG; p, passage.

ANDV/ARG large (L) segment. Coding-complete nucleic-acid sequences determined in this study were assessed together with previously determined sequences of ANDV, ANDV-like viruses Lechiguanas virus (LECV) and Orán virus (ORNV), BASV/BA02-C1S, and several American orthohantaviruses (Laguna Negra virus [LANV], Sin Nombre virus [SNV], Maporal virus [MAPV], Rio Mamoré virus [RIOMV], and Choclo virus [CHOV]). Four distinct ANDV clades are apparent in the most divergent S segment tree (Fig. 2B; details about the strains are listed in Table S1 in the supplemental material):

1. ANDV/CHI-7913 (Chile; long-tailed colilargo) and ANDV/NRC-4/18 (Argentina; human)
2. ANDV/Epilink/96, ANDV/Epuyén/18-19, ANDV/AREB14/P2 (Argentina, human; associated with person-to-person transmission) and ANDV/NCR-2/97 and ANDV/NRC-6/18 (Argentina, human)
3. ANDV/ARG (Argentina; long-tailed colilargo)
4. ANDV/CHI-9717869 (Chile; long-tailed colilargo).

ANDV/ARG is therefore not directly related to the other ANDV strains associated with person-to-person transmission. Interestingly, BASV clusters separately from ANDV *sensu stricto* together with LECV and ORNV; and, based on the analysis of the S, M, and L segments (Fig. S1), ANDV/CHI-9717869 appears to be the more ancestral strain. Furthermore, the analysis also shows that ANDV/ARG genetic distances to other strains reflect their geographic distribution (Fig. 2B).

Sequencing of passaged variants of Andes virus strain ARG reveals sites of adaptation associated with attenuation in the golden hamster model. To identify genotypic differences associated with golden hamster model outcome phenotype, we sequenced the S, M, and L genomic segments of ANDV/ARG p0 (sampled from the long-tailed colilargo). The resulting isolate was seeded in Vero E6 cells for analysis of p3, p9 (14), and p19, as well as lung-tissue homogenates from golden hamsters exposed to ANDV/ARG p9. We also included a human blood sample of Buenos Aires virus (BASV/BA02-C1S) from a case of HPS in La Plata, Provincia de Buenos Aires, in 2002 (21). We obtained complete genomic sequences for all segments (>98.3% coverage) for all ANDV strains, except for the L segment from the p0 strain (46.1% coverage). Sequences are available in GenBank under accession no. OP555720 to OP555735.

The comparative analysis revealed only a few nucleotide changes over passages (Table 1), and p0 and p3 sequences were identical. By p9, three single-nucleotide polymorphisms (SNPs) were observed: two in the S segment (S46N in the nucleocapsid [N] open reading frame [ORF] and V20I in the small nonstructural protein [NSs] [7] ORF) and one in the L segment (I1295M in the large protein [L] ORF). By p19, four additional SNPs were observed: two in the S segment, including a synonymous change at nucleotide position G57A and a nonsynonymous change at G103A (A21T), and two that were derived by nonsynonymous substitution, including one in the M segment (S97P), and one in the L segment (P1675S); also, one

Downloaded from https://journals.asm.org/journal/msphere on 06 June 2023 by 200.51.93.114.

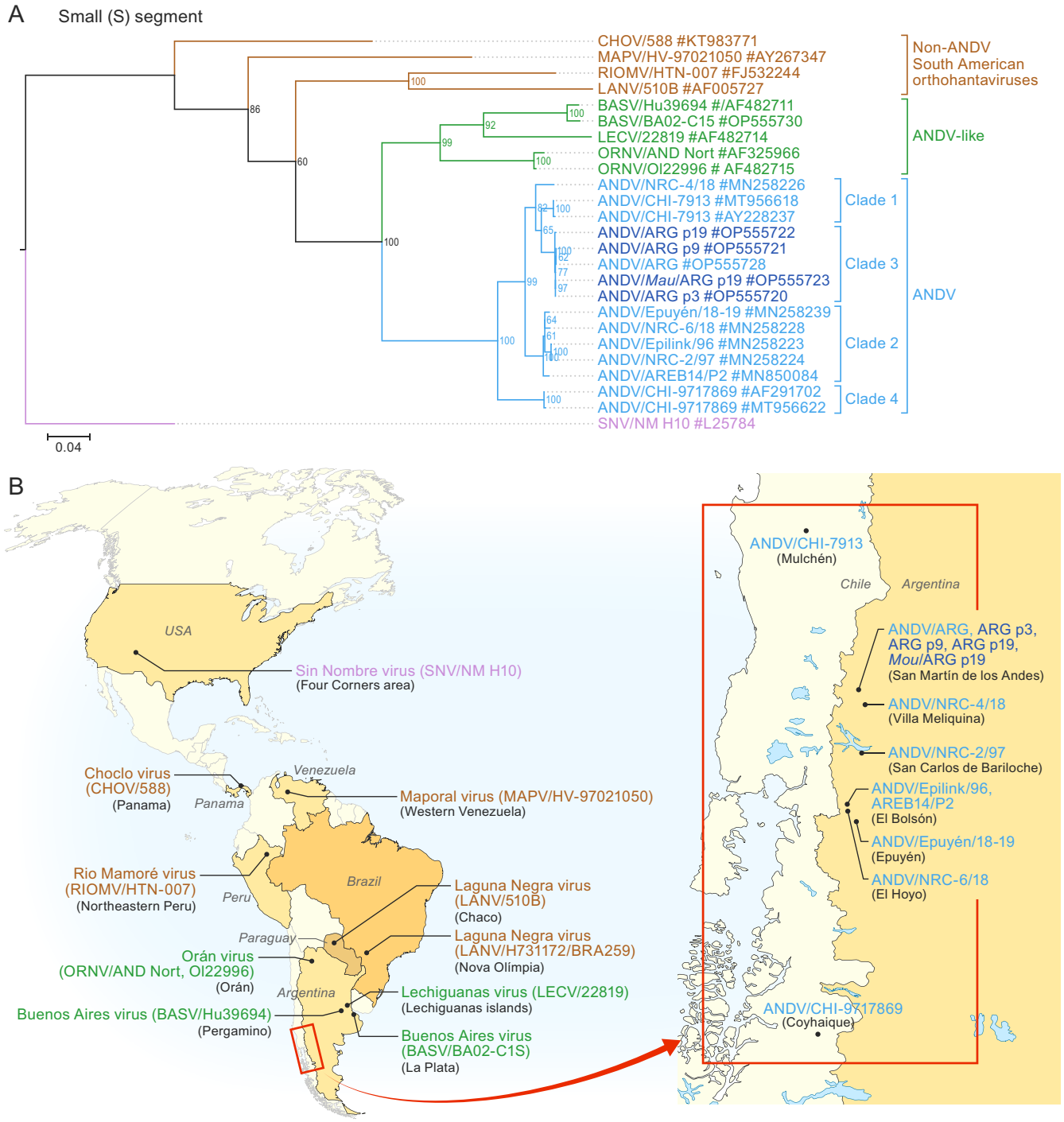

FIG 2 Phylogenetic analysis informs the evolutionary history of Buenos Aires virus (BASV) and Andes virus strain ARG (ANDV/ARG). (A) Small (S) segment analysis. Large (L) and medium (M) segment analyses are included in Fig. S1. All variants are listed with the strain name, region of origin, year of isolation, and accession number. Different colors are used for identification: brown for non-ANDV South American orthohantaviruses, green for ANDV-like viruses, light blue for ANDV strains in clades 1, 2, and 4, and some in clade 3, and dark blue for passaged strains in clade 3. Detailed information on epidemiological history of the strains is listed in Table S1. (B) Geographic distribution of American orthohantavirus strains analyzed in panel A. Mulchén and Coyhaique are in Chile; the other locations are in Argentina. The inset shows the area of endemicity of ANDV in Argentina and Chile.

reversion was observed in the S segment (affecting S46 in the N ORF and V20 in the small nonstructural protein [NSs] ORF). As expected, the p19 sequence had the highest number of nonsynonymous substitutions. The changes were predominantly transitions (87.5%). After correction by segment length, it is evident that most nucleotide substitutions accumulated in the S segment. Surprisingly, very few SNPs were observed in the M segment. Interestingly,

Downloaded from https://journals.asm.org/journal/msphere on 06 June 2023 by 200.51.93.114.

TABLE 1 Sequencing of passaged variants of ANDV/ARG reveals sites of adaptation associated with attenuation in the golden hamster model[a]

Genomic region	Position		ANDV passage in:					Type
				Cell culture				
	nt	aa	Rodent tissue; ARG p0	ARG p3	ARG p9	ARG p19	Infected golden hamster lungs; Mau/ARG p9	
S segment								
GenBank no.			OP555723	OP555720	OP555721	OP555722	OP555728	
N ORF	57	5	CAG (Q)	CAG (Q)	CAG (Q)	CA<u>A</u> (Q)	CAG (Q)	Syn
	103	21	GCT (A)	GCT (A)	GCT (A)	<u>A</u>CT (<u>T</u>)	GCT (A)	Nonsyn
	179	46	AGT (S)	AGT (S)	A<u>A</u>T (<u>N</u>)	AGT (S)	A<u>A</u>T (<u>N</u>)	Nonsyn
NCR	1488	Not coding	G	G	G	<u>T</u>	G	
NSs ORF (+1)	179	20	GTA (V)	GTA (V)	<u>A</u>TA (<u>I</u>)	GTA (V)	<u>A</u>TA (<u>I</u>)	Nonsyn
M segment								
GenBank no.			OP555724	OP555725	OP555726	OP555727	OP555729	
	337	97	TCC (S)	TCC (S)	TCC (S)	<u>C</u>CC (<u>P</u>)	TCC (S)	Nonsyn
L segment								
GenBank no.			NA	OP555732	OP555733	OP555734	OP555735	Functional region
	3557	1175	NA	ACC (T)	AC<u>T</u> (T)	AC<u>T</u> (T)	AC<u>T</u> (T)	Syn
	3919	1295	NA	ATA (I)	AT<u>G</u> (<u>M</u>)	AT<u>G</u> (<u>M</u>)	AT<u>G</u> (<u>M</u>)	Nonsyn
	5057	1675	NA	CCT (P)	CCT (P)	<u>T</u>CT (<u>S</u>)	CCT (P)	Nonsyn

[a]Underlined letters represent changes observed during passage. Abbreviations: Syn, synonymous; Nonsyn, nonsynonymous; NA, not available.

no reversions were detected in the genomic sequences of ANDV/ARG p9 in the lungs of golden hamsters exposed to ANDV/ARG p9. (Note that no data were collected from the lungs of golden hamsters exposed to ANDV/ARG p19).

Sequencing of Andes virus strain ARG reveals virulence markers compared with pathogenic and nonpathogenic strains of Andes virus utilized in the golden hamster model. To identify potential genotypic virulence markers in the ANDV/ARG genome, we initially focused on 23 specific SNPs that had been described between the golden hamster attenuated ANDV/CHI-7913 compared to golden hamster lethal ANDV/CHI-9717869 (17). We also mapped five additional SNPs between those genomes, as the NSs ORF was not included in the original comparison (17). In 23 of those 28 positions, ANDV/ARG p0 shared nucleotide bases with attenuated ANDV/CHI-7913. ANDV/CHI-97177869 and ANDV/ARG shared only position 11 of the Gn glycoprotein, position 938 of the Gc glycoprotein, and positions 20 and 37 of the NSs ORFs (Table 2). ANDV/ARG differ from both ANDV/CHI-7913 and ANDV/CHI-9717869 at genome position 46 of the N ORF.

Next, we focused on comparing the amino acid changes that arose during ANDV/ARG passaging with the differences in virulence observed in the golden hamster model. We identified five: A21T in the N ORF, V20I in the NSs ORF, S97P in the Gn glycoprotein, and I1295M and P1675S in the L ORF.

A21T, which appeared only in ANDV/ARG p19, occurs in a region known to participate in orthohantavirus NSs homotypic interactions (22). Additionally, we identified a second amino acid change in the N ORF (S46N), which was encoded only by ANDV/ARG p9 (Table 1 and Table 2). Interestingly, in the same N ORF, Simons et al. reported an ANDV-specific kinase-recruitable hypervariable domain (HVD) in the N ORF by comparison of ANDV/CHI-7913 with other American orthohantaviruses and demonstrated its importance in regulating interferon (IFN) signaling (23). The HVD, which consists of 44 residues (nucleotides 252 to 296), encodes six characteristic amino acids (at positions A253, K262, N273, H286, T289, and T296) that are determinants of the phosphorylation of S386 in the N ORF, which is posited as a virulence determinant (23). Although we confirmed that S386 and five of the six residues are conserved among all ANDV and ANDV-like viruses (Table 2 and Table 3), A253 is exclusive for ANDV, whereas P (BASV and LECV) or L (ORNV) is found in ANDV-like viruses; Q is found in MAPV, RIOMV, and LANV; and P is found in SNV and CHOV.

The recently discovered ANDV NSs antagonizes the type I IFN response by inhibiting mitochondrial antiviral-signaling protein (MAVS) signaling by binding MAV without disrupting MAVS-TBK-1 (22). In the presence of ANDV NSs, the ubiquitinylation of MAVS is reduced.

Downloaded from https://journals.asm.org/journal/msphere on 06 June 2023 by 200.51.93.114.

TABLE 2 Sequencing of ANDV/ARG reveals virulence markers compared with pathogenic and nonpathogenic strains of ANDV utilized in the golden hamster model[a]

Parameter	aa position	CHI-9717869	ANDV							Other orthohantavirus					Functional region	Note	Reference
			ARG				CHI-7913	Epuyén/18-19	Epilink/96	MAPV	RIOMV	LANV	SNV	CHOV			
			p0	p3	p9	p19											
Geographic origin		Coyhaique, Chile	SMA, Neuquén	SMA, Neuquén	SMA, Neuquén	SMA, Neuquén	Mulchén Biobío	Epuyén, Chubut	El bolsón, Río Negro	Western Venezuela	Peru	Chaco, Paraguay	United States	Panama			
Lethality in golden hamsters		High	High	High	High	Moderate	No	NA	NA	Moderate	No	NA	No	No			
Genomic region																	
S segment																	
GenBank no.		MT956622	OP555723	OP555720	OP555721	OP555722	MT956618	MN258239	MN258223	FJ008979	FJ532244	NC_038505	KT885046	KT983771			
N ORF	21	A	A	A	A	*T*	A	A	A	A	A	A	T	A	Homotypic interaction	ANDV attenuation	51, this work
	31	A	A	A	A	A	A	A	A	A	A	A	A	A	Coiled-coil region		This work
	38	D	D	D	D	D	D	D	D	D	D	D	D	E	Coiled-coil region		This work
	46	N	*S*	*S*	*N*	*S*	n	S	S	N	N	S	S	G	Coiled-coil bend	No	51, this work
	253	**A**	**A**	**A**	**A**	**A**	**A**	**A**	**A**	Q	Q	Q	P	P	HDV	ANDV exclusive	23
	262	**K**	**K**	**K**	**K**	**K**	**K**	**K**	**K**	R	R	R	R	R	HDV	ANDV exclusive	23
	273	**N**	**N**	**N**	**N**	**N**	**N**	**N**	**N**	R	D	D	D	R	HDV	ANDV exclusive	23
	286	**H**	**H**	**H**	**H**	**H**	**H**	**H**	**H**	T	A	A	D	T	HDV	ANDV exclusive	23
	289	**T**	**T**	**T**	**T**	**T**	**T**	**T**	**T**	A	S	A	A	S	HDV	ANDV exclusive	23
	296	**T**	**T**	**T**	**T**	**T**	**T**	**T**	**T**	H	N	N	A	K	HDV	ANDV exclusive	23
	386	**S**	**S**	**S**	**S**	**S**	**S**	**S**	**S**	H	F	S	H	H	Serine-kinase substrate	ANDV exclusive	23
NSs ORF (+1)	5	Q	R	R	R	R	R	R	R	Q	Q	Q	R	Q	Unknown		This work
	20	V	V	V	*I*	V	i	V	V	T	T	A	A	G	Unknown		This work
	33	E	G	G	G	G	G	G	G	G	Q	Q	E	E	Unknown		This work
	35	L	S	S	S	S	S	S	S	S	S	S	L	S	Unknown		This work
	37	G	G	G	G	G	d	G	G	G	D	G	G	G	Unknown	ANDV attenuation	This work
	40	Q	Q	Q	Q	Q	Q	**R**	**R**	Q	Q	Q	L	Q	Unknown	PTP outbreak related	This work
	47	N	N	N	N	N	N	**S**	**S**	N	S	N	N	N	Unknown	PTP outbreak related	This work
M segment																	
GenBank no.		MT956623	OP555724	OP555725	OP555726	OP555727	MT956619	MN258205	MN258194	AY363179	FJ608550	NC038506	L25783	KT983772			
	8	V	**A**	**A**	**A**	**A**	**A**	**A**	**A**	I	I	I	F	F	Signal sequence Gn	No	17
	11	V	V	V	V	V	i	V	V	V	V	V	V	V	Signal sequence Gn	ANDV attenuation	17
	97	S	S	S	S	*P*	S	S	S	A	A	S	A	A	Antibody epitope?	ANDV attenuation	This work
	294	H	**Y**	**Y**	**Y**	**Y**	**Y**	**Y**	**Y**	S	V	V	L	I	Interaction with Gc domain	No	17
	346	V	**I**	**I**	**I**	**I**	**I**	**I**	**I**	**I**	**I**	**I**	**I**	L	Gn domain B-near	No	17
	353	T	**V**	**V**	**V**	**V**	**V**	**I**	**I**	K	H	V	V	Q	Gn domain B-near	No	17
	499	V	V	V	V	V	V	**I**	**I**	L	L	L	L	L	Gn domain (?)-near	PTP outbreak related	This work
	537	I	**V**	**V**	**V**	**V**	**V**	**V**	**V**	**V**	**V**	**V**	**V**	I	Gn domain (?)-cytoplasmic	No	17
	569	**I**	**I**	**I**	**I**	**I**	**I**	**I**	**I**	P	A	V	P	C	Gn domain (?) cytoplasmic	ANDV exclusive	This work
	570	**N**	**N**	**N**	**N**	**N**	**N**	**N**	**N**	E	E	E	E	D	Gn domain (?)-cytoplasmic	ANDV exclusive	This work
	641	T	T	T	T	T	T	**I**	**I**	T	T	T	T	T	Gn domain (?)-near WASSA	PTP outbreak related	This work
	938	T	T	T	T	T	a	**A**	**A**	T	T	S	S	**A**	Gc domain II-near	No	17
	1023	T	A	A	A	A	A	A	A	T	A	A	T	V	Transmembrane doman Gc	No	17
	1115	V	V	V	V	V	V	**I**	**I**	V	V	V	**I**	V	?	PTP outbreak related	This work
	1133	**G**	**G**	**G**	**G**	**G**	**G**	**G**	**G**	S	S	S	S	V	Gc cytoplasmic tail-RNP-	ANDV exclusive	This work
L segment																	
GenBank no.		MT956621	NA	OP555732	OP555733	OP555734	MT956620	MN258188	MN258156	EU788002	FJ809772	JX443696	L37901	EF397003			
	141	T	NA	**I**	**I**	**I**	**I**	V	V	I	I	**I**	Q	Q	Endonuclease domain	No	17
	181	I	NA	V	V	V	V	V	V	V	V	V	V	V	Unknown		17
	277	L	NA	**S**	**S**	**S**	**S**	**S**	**S**	E	E	E	V	L	Unknown	No	17
	338	S	NA	**A**	**A**	**A**	**A**	**A**	**A**	A	**A**	**A**	**A**	**A**	Unknown	No	17
	346	R	NA	**K**	**K**	**K**	**K**	**K**	**K**	R	**E**	**K**	R	R	Unknown	No	17
	402	I	NA	**V**	**V**	**V**	**V**	I	I	T	M	I	P	I	Unknown	No	17
	780	D	NA	**N**	**N**	**N**	**N**	**N**	**N**	E	K	V	Q	Q	Unknown	No	17
	1033	N	NA	**D**	**D**	**D**	**D**	**D**	**D**	**D**	**D**	E	E	N	Unknown	No	17
	1252	T	NA	T	T	T	**T**	T	T	I	T	T	V	T	Unknown		17
	1295	I	NA	I	*M*	*M*	I	I	I	I	I	I	Y	I	Unknown	No	This work
	1303	D	NA	**E**	**E**	**E**	**E**	**E**	**E**	D	D	D	D	D	Unknown	No	17
	1665	V	NA	**I**	**I**	**I**	**I**	V	V	I	**I**	**I**	V	V	Unknown	No	17

(Continued on next page)

Downloaded from https://journals.asm.org/journal/msphere on 06 June 2023 by 200.51.93.114.

TABLE 2 (Continued)

Parameter	aa position	CHI-9717869	ANDV							Other orthohantavirus					Functional region	Note	Reference
			ARG				CHI-7913	Epuyén/18-19	Epilink/96	MAPV	RIOMV	LANV	SNV	CHOV			
			p0	p3	p9	p19											
	1675	P	NA	P	P	*S*	P	P	P	P	P	P	P	P	Unknown	ANDV atenuation	This work
	1750	K	NA	**R**	**R**	**R**	**R**	**R**	**R**	K	K	R	K	R	Unknown	No	17
	1828	T	NA	P	P	P	P	P	P	P	P	P	A	P	Unknown		17
	2109	I	NA	**V**	**V**	**V**	**V**	**V**	**V**	R	R	R	N	T	Unknown	No	17
	2113	T	NA	**A**	**A**	**A**	**A**	T	T	K	T	T	R	A	Unknown	No	17

[a]Lowercase letters represent SNPs that differentiate ANDV/CHI-7913 and ANDV/CHI-917869, where ANDV/ARG segregates with ANDV/CHI-7913. Underlined letters represent SNPs that differentiate ANDV/CHI-7913 and ANDV/CHI-917869, where ANDV/ARGs segregate with ANDV/CHI-9177869. Italic letters represent SNPs selected during passaging. Boldface underlined letters represent SNPs that characterize PTP isolates. Italic underlined letters represent SNPs that are unique to ANDV/ARG (not present in ANDV/CHI-7913 nor in ANDV/CHI-9177869). Boldface letters are only included for emphasis. Abbreviations: HPV, kinase recruitment site; NA, not available.

Downloaded from https://journals.asm.org/journal/msphere on 06 June 2023 by 200.51.93.114.

TABLE 3 Sequencing of ANDV/ARG reveals potential transmissibility markers when comparing ANDV strains with differences of efficiency in person-to-person potential[a]

	ANDV										BASV			
Parameter	CHI-9717869	ARG	Epuyén/18-19	Epilink/96	AREB14/P2	NRC-6/18	NRC-4/18	NRC-2/97	NRC-4/97	CHi-7913	BA02-C1S	Hu39694	LECV 22819	ORNV and nort
Country	Chile	Argentina	Argentina	Argentina	Argentina	Argentina	Argentina	Argentina	Argentina	Chile	Argentina	Argentina	Argentina	Argentina
Geographic origin	Coyhaique	SMA, Neuquén	Epuyén, Chubut	El bolsón, Río Negro	El bolsón, Río Negro	El hoyo, Chubut	Villa meliquina, Neuquén	Bariloche, Río Negro	Villa meliquina, Neuquén	Mulchén, BioBío	La plata, BsAs	Pergamino, BsAs	BsAs	Orán, Salta
Source	Rodent	Rodent	Human	Human	Human	Human	Human	Human	Human	Human	Human	Human	Rodent	Rodent
Clade	4	3	2	2	2	2	1	1	1	1	ANDV-like	ANDV-like	ANDV-like	ANDV-like
Person-to-person transmission	No	-	Outbreak (n = 34)	Outbreak (n = 16)	Outbreak (n = 3)	No	Event	No	No	No	Event	No	No	No
Genomic region (aa position)														
S segment														
GenBank no.	MT956622	OP555720	MN258239	MN258223	MN850084	MN258228	MN258225	MN258224	MN258226	MT956618	OP555730	AF482711	AF482714	AF325966
N														
31	A	A	A	A	A	A	A	A	A	A*	*T*	*T*	*T*	*T*
38	D	D	D	D	D	D	D	D	D	D*	*E*	*E*	*E*	*E*
253	**A**	**A**	**A**	**A**	**A**	**A**	**A**	**A**	**A**	**A**	*P*	*P*	*P*	*L*
262	K	K	K	K	K	K	K	K	K	K	K	K	K	K
273	N	N	N	N	N	N	N	N	N	N	N	N	N	N
286	H	H	H	H	H	H	H	H	H	H	H	H	H	H
289	T	T	T	T	T	T	T	T	T	T^	T	T	T	I
296	T	T	T	T	T	T	T	T	T	T	T	T	T	T
386*	S	S	S	S	S	S	S	S	S	S	S	S	S	S
NSs														
5	Q	R	R	R	R	R	R	R	R	R	R	R	R	R
20	V	V	V	V	V	V	V	V	V	i	**V**	**V**	**V**	**V**
33	E	G	G	G	G	G	G	G	G	G	E	E	G	E
35	L	S	S	S	S	S	S	S	S	S	S	S	S	L
37	G	G	G	G	G	G	G	G	G	d	**G**	**G**	**D**	**G**
40	Q	Q	**R**	**R**	**R**	**R**	Q	Q	Q	Q	P	P	Q	R
47	N	N	**S**	**S**	**S**	**S**	N	N	N	N	N	N	N	N
M segment														
GenBank no.	MT956623	OP555725	MN258205	MN258189	MN850089	MN258194	MN258191	MN258190	MN258192	MT956619	OP555731	AF028023	AF028022	AF028024
M														
499	V	V	I	I	I	I	V	V	V	V	I	I	I	I
569	I	I	I	I	I	I	I	I	I	I	I	I	I	I
570	N	N	N	N	N	N	N	N	N	N	N	N	N	N
641	T	T	**I**	**I**	**I**	**I**	T	T	T	T	T	T	T	T
1133	G	G	G	G	G	G	G	G	G	G	G	G	G	G

[a]Lowercase letters represent SNPs that differentiate ANDV/CHI-7913 and ANDV/CHI-917869, where ANDV/ARG segregates with ANDV/CHI-7913. Underlined letters represent SNPs that differentiate ANDV/CHI-7913 and ANDV/CHI-917869, where ANDV/ARG segregates with ANDV/CHI-9177869. Boldface underlined letters represent SNPs that characterize PTP isolates. Italic letters represent SNPs that differentiate ANDV-like from ANDV viruses. Boldface letters are only included for emphasis. *, SNPs (likely sequencing errors) in AF325966.

Downloaded from https://journals.asm.org/journal/msphere on 06 June 2023 by 200.51.93.114.

The V20I SNPs in the NSs ORF were observed arising in the ANDV/ARG p9 strain by the same mutation at nucleotide position 179 in the S segment. (Note that the NSs ORF is at position +1 compared with the N ORF.) ANDV/CHI-9717869 and ANDV/CHI-7913 differ in the NSs ORF at five amino acid positions (5, 20, 33, 35, and 37) (Table 2 and Table 3).

The S97P Gn change, found only in ANDV/ARG p19, could not be associated with any functional change. The site has only been reported as part of an antibody epitope (24). The S residue is conserved in BASV and LANV Gn proteins, whereas other orthohantavirus Gn proteins (LECV, ORNV, MAPV, RIOMV, SNV, and CHOV) have an A at that position (Table 2).

M1295 and S1675 in the L ORF were encoded by ANDV/ARG p9 and p19 strains, respectively, but those genomic regions could not be associated with any functionality. M1295 has not been observed previously in nature; other orthohantaviruses have I1295 (MAPV, RIOMV, LANV, and CHOV) or Y1295 (SNV) (Table 2). S1675 has not been observed in L ORFs of other orthohantaviruses, and the P1675 position appears entirely conserved (Table 2).

Sequencing of Andes virus strain ARG reveals potential transmissibility markers when comparing Andes virus strains with differences of efficiency in person-to-person potential. The presence of outbreak-related determinants associated with person-to-person transmission was assessed by comparing genomic sequences of ANDV strains from clades clearly associated with person-to-person transmission and ANDV strains and ANDV-like viruses (BASV, LECV, and ORNV) that had not (Table 3). Interestingly, BASV, the most closely related ANDV-like virus (Fig. 2A and B), has also been implicated in secondary transmissions but with limited efficiency (21, 25).

Only one mutation in the M segment (resulting in T641I) was unique to person-to-person-associated clade 2 strains. Only one mutation in the S segment (resulting in A253N) was exclusively present in ANDV, whereas S386 is conserved among ANDV strains and ANDV-like viruses. Our analysis did not include the L segment of ANDV-like viruses because those sequences remain unavailable.

Five M ORF positions were unique to ANDV genomes compared with genomes of American orthohantaviruses (amino acid residue positions 499, 569, 570, 641, and 1133) (Table 2). Four positions (569, 570, 641, and 1133) are also shared by ANDV-like viruses (Table 3). S97 is encoded by all ANDV strains and BASV. V499I was present in some PTP strains and also in ANDV-like strains, whereas the T641I change was only encoded by ANDV strains from the clade associated with person-to-person transmission. However, only the latter (T641I) had been mapped in the vicinity of the absolutely conserved pentapeptide WAASA cleavage site, where signal peptidases cleave Gn and Gc (26). Since position 641 maps to a region that provides a signal to cellular peptidases, this change might affect the cleavage's efficiency. Signal peptides share several characteristic features determined by their amino acid composition (27), including a tripartite architecture with a positively charged N terminus and a hydrophobic segment that determines the strength of the signal. T641 changes from a polar noncharged amino acid (T) to a nonpolar (I) amino acid.

In comparison with the bulk of described ANDV isolates, the recently discovered ANDV NSs ORF presents seven sites of variation. Three are unique to ANDV/CHI-9717869 (Q5, E33, and L35) and two are unique to ANDV/CHI-7913 (I20 and D37). Intriguingly, we identified two SNPs in the NSs ORF at positions 40 (Q40R) and 47 (N47S) that were present only in the clade 2 strains (e.g., ANDV/Epuyén/18-19 and ANDV/Epilink/96) associated with person-to-person transmission. Both NSs ORF changes need to be functionally evaluated for their effect on MAVS signaling.

DISCUSSION

Passaging in cell culture, especially when involving different hosts, usually results in virus adaptation, often affecting their virulence (19, 28, 29). However, ANDV/ARG p0 and p3 genome sequences were identical, and very few mutations were accumulated in the p9, p19, and hamster strains. The two amino acid substitutions (A21T and S46N) in N mapped to the intramolecular coiled-coil structure in the N-terminal region (α1 and α2), an exceptionally well-conserved region implicated in antibody recognition, formation of the ribonucleoprotein complex, and genome encapsidation (30–33). Interestingly, one adaptation appears to involve a change in NSs, which has been recently related to IFN regulation. Only

Downloaded from https://journals.asm.org/journal/msphere on 06 June 2023 by 200.51.93.114.

a single nucleotide change (T337C) was found in the M segment during late passaging (p19). This is unexpected since the M segment encodes Gn and Gc, two of the most variable regions of the genome in evolutionary terms.

Interestingly, we could also correlate some of the changes with differences in virulence in a small-animal model. ANDV/ARG p9 is uniformly lethal in hamsters (14). However, ANDV/ARG p19 was significantly less lethal (66.4%). Compared side by side, the ANDV/ARG p9 and p19 only diverged in five encoded residues (A21T and N46S in N, I20V in NSs, S97P in Gn, and P1675S in RNA-directed RNA polymerase [RdRp] encoded by the S, M, and L segments, respectively). Nevertheless, based on previous knowledge of functional domains, only the changes in N had been associated with viral replication. Structural studies of the N-terminal region of SNV and ANDV demonstrated that basic residues interact with the N core to stabilize interprotomer N association and formation of ribonucleoprotein (RNP) complexes (32). The A21T change likely affects that region, which is exceptionally well conserved among orthohantaviruses. The region is a target of the most cross-reactive antibodies against orthohantavirus, immunodominant, and proposed to have important effects regarding N polymerization, RNP complex formation, and subcellular localization of the assembly sites (30–32). We hypothesize that A21T and other changes in N (Table 2 and Table 3) may affect N oligomerization dynamics. The importance of this area as a potential determinant of pathogenesis might be underscored by the observed differences in the region at positions 31 (A31T) and 38 (D38E) (Table 3) that define ANDV-like viruses (i.e., BASV, LECV, and ORNV). The changes, all located at the bend between the two parallel coiled regions, could potentially affect the structure of the region. On the other hand, these two changes are only encoded by ANDV-like viruses, but not by LANV, MAPV, RIOMV, or SNV (Table 2). Thus, if these markers are associated with virulence, they would act via changes in the structure and not necessarily by SNP differences. Although the A21T change observed in late passages of ANDV/ARG is intriguing, A21 is conserved in BASV, LECV, and ORNV, but not SNV (Table 2). Collectively, this could indicate that structural changes in this area could be driving virulence differences instead of SNPs. Nonetheless, the limited animal data presented here could be improved with the use of imaging, advanced histological analyses, and other multiomics technologies. Support from developing countries and funding agencies for the study of these neglected pathogens is urgently needed as the resources for these types of studies in low- or middle-income countries (LMICs) are lacking.

Moreover, our analysis confirmed that the amino acid position S386, previously posited by Simons as a determinant of virulence (23), is conserved by ANDV, ANDV-like viruses (BASV, LECV, and ORNV), and LANV. In the N HVD, all ANDV strains share the described signature six residues, which are not found in any other orthohantavirus N HVD (Table 2). However, only five residues are shared with the three ANDV-like viruses, whereas A253 seems to be an exclusive ANDV marker (Table 3). We therefore suggest that A253 is an ANDV-exclusive virulence determinant and that the S386 modification and the five remaining HDV residues are virulence determinants for all viruses currently classified in the species *Andes orthohantavirus* (i.e., ANDV and ANDV-like viruses). However, based on the differences in lethality in hamsters among ANDV/CHI-9713 (nonlethal in golden hamsters), LANV (nonlethal in Brandt's hamsters [*Mesocricetus brandti* (Nehring, 1898)]) (34), MAPV (moderately lethal in golden hamsters), and ANDV/CHI-9717869 and ANDV/ARG (highly lethal in golden hamsters), the change in S386 does not appear to be a virulence determinant in hamsters. The N ORF has been associated with multiple functions associated with pathogenesis and virulence. The efficiency of orthohantavirus replication is inversely proportional to the ability of infected cells to activate MxA expression (35). The MxA protein is a critical component of the antiviral state induced by type I IFN (36). In turn, MxA protein binds to N, forming an MxA-N protein complex in a yet-to-be-defined manner (37). Moreover, the N protein also has a role in regulating the antiviral state. For instance, ANDV N hinders autophosphorylation of TBK1, resulting in the inhibition of interferon regulatory factor 3 (IRF3) phosphorylation and RIG-I/MDA5-directed type I IFN induction (38). Additionally, N can affect protein kinase R (PKR) dimerization (39), thereby

Downloaded from https://journals.asm.org/journal/msphere on 06 June 2023 by 200.51.93.114.

preventing PKR phosphorylation, which is essential for its enzymatic activity. PKR inhibits virus replication (40).

Bunyaviral NSs are nonessential for virus replication, but they are pathogenesis determinants by acting as IFN antagonists (41). As a case in point, ANDV/CHI-9717869 NSs antagonize the type I IFN induction pathway (22). We therefore hypothesize that the two changes observed in NSs of ANDV strains associated with person-to-person transmission might enhance IFN antagonist potential. Moreover, the number of changes in ANDV/CHI-9717869 compared with ANDV/CHI-7913 and ANDV/ARG might explain the differences in lethality in the golden hamster animal model.

In the M segment, the amino acid change T641I is also shared among ANDV strains associated with person-to-person-transmission but not among ANDV-like viruses. However, the change is also found in ANDV/NRC-6/18, which has not been associated with person-to-person transmission, and it is absent in ANDV/NRC-3/18, which has been involved in an event of secondary transmission (Table 3). T641 is located in the signal peptide of Gc, in the region preceding the hyperconserved cleavage site WAASA. Because host protease binding sites are guided by the signal from this region (22), we hypothesize that this change might affect the dynamics and speed of ANDV glycoprotein retention and trafficking. Signal peptides share several characteristic features determined by their amino acid composition (42), including a tripartite architecture with a positively charged N terminus and a hydrophobic segment that determines the strength of the signal. The comparative data presented here need to be complemented experimentally. For instance, recombinant vesicular stomatitis Indiana viruses expressing orthohantavirus glycoproteins could be used to partially compensate for the current lack of reverse-genetics systems for orthohantaviruses (43).

The phylogenetic analysis showed that ANDV/ARG is closely related to variants causing disease in humans and groups according to their geographic origin. ANDV/CHI-7913 is most closely related to ANDV/ARG, more than sequences obtained from patients reported in the region of endemicity. ANDV/CHI-9717869, on the other hand, is the most genetically divergent and remote geographically. Indeed, ANDV/ARG and ANDV/CHI-7913 share the most positions compared to ANDV/CHI-9717869. Thus, the decision to use ANDV/CHI-9717869 as the accepted exposure stock for medical countermeasure assessment needs to be revised, as this strain is a clear outlier that might not be representative of wild-type circulating strains.

Taken together, the results of our study indicate that determination and subsequent comparison of wild-type, cell-culture-passaged, and animal model-derived ANDV—and likely other orthohantavirus genome sequences—may allow predictions regarding their overall virulence and transmissibility, possibly informing countermeasure approaches. To strengthen such predictions, additional sequence information from yet-to-be-characterized ANDV strains and completion of genomic sequences of ANDV-like viruses are warranted.

MATERIALS AND METHODS

Viruses and cells. Andes virus strain ARG (ANDV/ARG) was isolated from a long-tailed colilargo (*Oligoryzomys longicaudatus* (Bennett, 1832)) in grivet [*Chlorocebus aethiops* (Linnaeus, 1758)] kidney epithelial Vero E6 cells (CRL-1586; ATCC, Manassas, VA, USA) (20). Continuous ANDV infection of cells was monitored by immunofluorescence performed with a rabbit polyclonal serum generated against ANDV nucleocapsid protein (N) open reading frame (ORF) and real-time reverse transcription-quantitative PCR (RT-qPCR), and cultures were passaged blindly. Serial passaging (p9 to p19) was performed at a multiplicity of infection of 0.1.

Pathogenicity assessment. An established lethal animal model of ANDV infection, using golden hamsters [*Mesocricetus auratus* (Waterhouse, 1839)] (12), was leveraged to compare the previously established pathogenicity of the ANDV strain ARG (ANDV/ARG p9) (17) and to assess the pathogenicity of ANDV/ARG p19. Eight 12-week-old golden hamsters (four males and four females, obtained from the Instituto Nacional de Producción de Biológicos in Buenos Aires) were exposed intramuscularly to 100 μL of mock inoculum (phosphate-buffered saline [PBS]). Nine 12-week-old golden hamsters (four males and five females) were exposed intramuscularly to 100 μL of PBS containing 10^5 focus-forming units (FFU) of ANDV/ARG p19. Exposed golden hamsters were placed individually in ventilated cages and monitored daily up to 33 days postexposure. Food and water were available *ad libitum*. All animal experiments were performed in an accredited animal biological safety level 3 ABSL-3 biocontainment laboratory in compliance with institutional guidelines and Argentinian national law no. 14,346, which regulates experiments involving animals

Downloaded from https://journals.asm.org/journal/msphere on 06 June 2023 by 200.51.93.114.

and adheres to principles stated in the *Guide for the Care and Use of Laboratory Animals* (44) of the National Research Council. An Institutional Animal Care and Use Committee approved all procedures involving animals.

RT-qPCR. Lung specimens were obtained from all golden hamsters following standard necropsy protocols. Total RNA was extracted from lung specimens using TRIzol, as described previously (45). RT-qPCR using ANDV genomic small (S) segment primers was performed following published procedures (46). Two microliters of each RNA sample were amplified in duplicate assays with a CFX detection system (Bio-Rad, Hercules, CA, USA), using TaqMan RT-PCR master mix (Quanta Biosciences, Gaithersburg, MD, USA), according to the manufacturers' instructions. A primer set designed to detect the human RNase P gene was used to ensure that samples were free of PCR inhibitors and that RNA extractions were homogeneous.

Genomic and phylogenetic analyses. Virus genome sequencing was performed using three ANDV cell culture passages (early [p3], intermediate [p9], and late [p19]), cryopreserved lung tissue from a naturally ANDV-infected long-tailed colilargo (p0), and lung tissues obtained from golden hamsters exposed to ANDV/ARG p9. Also included in the analysis was a blood clot sample from a HPS patient (case C1-s, survivor, 14 years old) associated with secondary transmission of Buenos Aires virus (BASV) in Central Argentina (21).

Total RNA was extracted from cell culture supernatants, lung tissues, and clinical samples utilizing TRIzol. Virus genome sequencing was performed as previously described (11, 47). Briefly, a targeted bait-enrichment approach was used to enrich transcriptome sequencing (RNA-seq) libraries for sequencing on the MiSeq platform (Illumina, San Diego, CA, USA). Orthohantavirus sequences from each genomic segment (S, M, and L) were collected (Table S1) and aligned using MAFFT v.7.397, implemented in ClustalW version 2.0 (48). The initial data set consisted of coding-complete sequences obtained in this work and listed in Table S1. Other American orthohantavirus sequences from GenBank were also included. The resulting alignments were visually inspected to identify synonymous and nonsynonymous changes. Phylogenetic trees were reconstructed using IQ-TREE v.1.6.12 (49) with automatic model selection (50). Branch supports were assessed by 1,000 ultrafast bootstraps (49).

Data availability. Sequencing data are publicly available through GenBank under accession no. OP555720 to OP555735.

SUPPLEMENTAL MATERIAL

Supplemental material is available online only.

FIG S1, EPS file, 1.3 MB.

TABLE S1, XLSX file, 0.01 MB.

ACKNOWLEDGMENTS

We gratefully acknowledge Silvia A. Girard for excellent technical assistance, M. Amoroso for veterinary medical care, and Alexis Edelstein for access to the animal biological safety level 3 facilities. We also thank Anya Crane (Integrated Research Facility at Fort Detrick, National Institute of Allergy and Infectious Diseases, National Institutes of Health, Fort Detrick, Frederick, MD, USA) for critically editing the manuscript and Jiro Wada (Integrated Research Facility at Fort Detrick, National Institute of Allergy and Infectious Diseases, National Institutes of Health, Fort Detrick, Frederick, MD, USA) for preparing figures.

This work was supported mainly by institutional funds of ANLIS "Dr. Carlos G. Malbran" as well as institutional funds to the Palacios Laboratory by the Icahn School of Medicine at Mount Sinai. This work was also supported in part through Laulima Government Solutions, LLC, prime contract with the National Institutes of Health (NIH) National Institute of Allergy and Infectious Diseases (NIAID) under contract no. HHSN272201800013C. J.H.K. performed this work as an employee of Tunnell Government Services (TGS), a subcontractor of Laulima Government Solutions, LLC, under contract no. HHSN272201800013C. The views and conclusions contained in this document are those of the authors and should not be interpreted as necessarily representing the official policies, either expressed or implied, of the U.S. Department of Health and Human Services, the U.S. Army, or of the institutions and companies affiliated with the authors, nor does mention of trade names, commercial products, or organizations imply endorsement by the U.S. Government.

We declare no conflict of interest.

REFERENCES

1. Kuhn JH, Charrel RN. 2018. Arthropod-borne and rodent-borne virus infections, p 1489–1509. *In* Jameson JL, Fauci AS, Kasper DL, Hauser SL, Longo DL, Loscalzo J (ed), Harrison's principles of internal medicine, 20th ed, vol 2. McGraw-Hill Education, Columbus, OH.
2. Alonso DO, Iglesias A, Coelho R, Periolo N, Bruno A, Córdoba MT, Filomarino N, Quipildor M, Biondo E, Fortunato E, Bellomo C, Martínez VP. 2019. Epidemiological description, case-fatality rate, and trends of hantavirus pulmonary syndrome: 9 years of surveillance in Argentina. J Med Virol 91:1173–1181. https://doi.org/10.1002/jmv.25446.
3. Martinez VP, Bellomo CM, Cacace ML, Suárez P, Bogni L, Padula PJ. 2010. Hantavirus pulmonary syndrome in Argentina, 1995–2008. Emerg Infect Dis 16:1853–1860. https://doi.org/10.3201/eid1612.091170.

Downloaded from https://journals.asm.org/journal/msphere on 06 June 2023 by 200.51.93.114.

4. Wells RM, Sosa Estani S, Yadon ZE, Enria D, Padula P, Pini N, Mills JN, Peters CJ, Segura EL, Hantavirus Pulmonary Syndrome Study Group for Patagaonia. 1997. An unusual hantavirus outbreak in southern Argentina: person-to-person transmission? Emerg Infect Dis 3:171–174. https://doi.org/10.3201/eid0302.970210.
5. Tortosa F, Carrasco G, Gallardo D, Prandi D, Parodi V, Santamaría G, Ragusa M, Volij C, Izcovich A. 2022. Factores pronósticos de síndrome cardiopulmonar y muerte por hantavirus Andes Sur: estudio de cohorte en San Carlos de Bariloche y su zona de influencia sanitaria. Medicina (B Aires) 82:351–360.
6. Levis S, Morzunov SP, Rowe JE, Enria D, Pini N, Calderon G, Sabattini M, St Jeor SC. 1998. Genetic diversity and epidemiology of hantaviruses in Argentina. J Infect Dis 177:529–538. https://doi.org/10.1086/514221.
7. Jonsson CB, Schmaljohn CS. 2001. Replication of hantaviruses. Curr Top Microbiol Immunol 256:15–32.
8. Padula PJ, Edelstein A, Miguel SDL, López NM, Rossi CM, Rabinovich RD. 1998. Brote epidémico del síndrome pulmonar por hantavirus en la Argentina. Evidencia molecular de la transmisión persona a persona del virus Andes. Medicina (B Aires) 58(Suppl 1):27–36.
9. Enria D, Padula P, Segura EL, Pini N, Edelstein A, Posse CR, Weissenbacher MC. 1996. Hantavirus pulmonary syndrome in Argentina. Possibility of person to person transmission. Medicina (B Aires) 56:709–711.
10. Riquelme R, Rioseco ML, Bastidas L, Trincado D, Riquelme M, Loyola H, Valdivieso F. 2015. Hantavirus pulmonary syndrome, Southern Chile, 1995–2012. Emerg Infect Dis 21:562–568. https://doi.org/10.3201/eid2104.141437.
11. Martínez VP, Di Paola N, Alonso DO, Pérez-Sautu U, Bellomo CM, Iglesias AA, Coelho RM, López B, Periolo N, Larson PA, Nagle ER, Chitty JA, Pratt CB, Díaz J, Cisterna D, Campos J, Sharma H, Dighero-Kemp B, Biondo E, Lewis L, Anselmo C, Olivera CP, Pontoriero F, Lavarra E, Kuhn JH, Strella T, Edelstein A, Burgos MI, Kaler M, Rubinstein A, Kugelman JR, Sanchez-Lockhart M, Perandones C, Palacios G. 2020. "Super-spreaders" and person-to-person transmission of Andes virus in Argentina. N Engl J Med 383:2230–2241. https://doi.org/10.1056/NEJMoa2009040.
12. Hooper JW, Larsen T, Custer DM, Schmaljohn CS. 2001. A lethal disease model for hantavirus pulmonary syndrome. Virology 289:6–14. https://doi.org/10.1006/viro.2001.1133.
13. Milazzo ML, Eyzaguirre EJ, Molina CP, Fulhorst CF. 2002. Maporal viral infection in the Syrian golden hamster: a model of hantavirus pulmonary syndrome. J Infect Dis 186:1390–1395. https://doi.org/10.1086/344735.
14. Martinez VP, Padula PJ. 2012. Induction of protective immunity in a Syrian hamster model against a cytopathogenic strain of Andes virus. J Med Virol 84:87–95. https://doi.org/10.1002/jmv.22228.
15. Toro J, Vega JD, Khan AS, Mills JN, Padula P, Terry W, Yadón Z, Valderrama R, Ellis BA, Pavletic C, Cerda R, Zaki S, Shieh W-J, Meyer R, Tapia M, Mansilla C, Baro M, Vergara JA, Concha M, Calderon G, Enria D, Peters CJ, Ksiazek TG. 1998. An outbreak of hantavirus pulmonary syndrome, Chile, 1997. Emerg Infect Dis 4:687–694. https://doi.org/10.3201/eid0404.980425.
16. Galeno H, Mora J, Villagra E, Fernandez J, Hernandez J, Mertz GJ, Ramirez E. 2002. First human isolate of hantavirus (Andes virus) in the Americas. Emerg Infect Dis 8:657–661. https://doi.org/10.3201/eid0807.010277.
17. Warner BM, Sloan A, Deschambault Y, Dowhanik S, Tierney K, Audet J, Liu G, Stein DR, Lung O, Buchanan C, Sroga P, Griffin BD, Siragam V, Frost KL, Booth S, Banadyga L, Saturday G, Scott D, Kobasa D, Safronetz D. 2021. Differential pathogenesis between Andes virus strains CHI-7913 and Chile-9717869 in Syrian hamsters. J Virol 95:e00108-21. https://doi.org/10.1128/JVI.00108-21.
18. Safronetz D, Prescott J, Feldmann F, Haddock E, Rosenke R, Okumura A, Brining D, Dahlstrom E, Porcella SF, Ebihara H, Scott DP, Hjelle B, Feldmann H. 2014. Pathophysiology of hantavirus pulmonary syndrome in rhesus macaques. Proc Natl Acad Sci U S A 111:7114–7119. https://doi.org/10.1073/pnas.1401998111.
19. Nemirov K, Lundkvist Å, Vaheri A, Plyusnin A. 2003. Adaptation of Puumala hantavirus to cell culture is associated with point mutations in the coding region of the L segment and in the noncoding regions of the S segment. J Virol 77:8793–8800. https://doi.org/10.1128/jvi.77.16.8793-8800.2003.
20. Padula PJ, Sanchez AJ, Edelstein A, Nichol ST. 2002. Complete nucleotide sequence of the M RNA segment of Andes virus and analysis of the variability of the termini of the virus S, M and L RNA segments. J Gen Virol 83:2117–2122. https://doi.org/10.1099/0022-1317-83-9-2117.
21. Martinez VP, Bellomo C, San Juan J, Pinna D, Forlenza R, Elder M, Padula PJ. 2005. Person-to-person transmission of Andes virus. Emerg Infect Dis 11:1848–1853. https://doi.org/10.3201/eid1112.050501.
22. Vera-Otarola J, Solis L, Lowy F, Olguín V, Angulo J, Pino K, Tischler ND, Otth C, Padula P, López-Lastra M. 2020. The Andes orthohantavirus NSs protein antagonizes the type I interferon response by inhibiting MAVS signaling. J Virol 94:e00454-20. https://doi.org/10.1128/JVI.00454-20.
23. Simons MJ, Gorbunova EE, Mackow ER. 2019. Unique interferon pathway regulation by the Andes virus nucleocapsid protein Is conferred by phosphorylation of serine 386. J Virol 93:e00338-19. https://doi.org/10.1128/JVI.00338-19.
24. Duehr J, McMahon M, Williamson B, Amanat F, Durbin A, Hawman DW, Noack D, Uhl S, Tan GS, Feldmann H, Krammer F. 2020. Neutralizing monoclonal antibodies against the Gn and the Gc of the Andes virus glycoprotein spike complex protect from virus challenge in a preclinical hamster model. mBio 11:e00028-20. https://doi.org/10.1128/mBio.00028-20.
25. Iglesias AA, Bellomo CM, Martínez VP. 2016. Síndrome pulmonar por hantavirus en Buenos Aires, 2009–2014. Medicina (B Aires) 76:1–9.
26. Löber C, Anheier B, Lindow S, Klenk H-D, Feldmann H. 2001. The Hantaan virus glycoprotein precursor is cleaved at the conserved pentapeptide WAASA. Virology 289:224–229. https://doi.org/10.1006/viro.2001.1171.
27. von Heijne G. 1990. The signal peptide. J Membr Biol 115:195–201. https://doi.org/10.1007/BF01868635.
28. Koehler A, Kolesnikova L, Becker S. 2016. An active site mutation increases the polymerase activity of the guinea pig-lethal Marburg virus. J Gen Virol 97:2494–2500. https://doi.org/10.1099/jgv.0.000564.
29. Trefry JC, Wollen SE, Nasar F, Shamblin JD, Kern SJ, Bearss JJ, Jefferson MA, Chance TB, Kugelman JR, Ladner JT, Honko AN, Kobs DJ, Wending MQS, Sabourin CL, Pratt WD, Palacios GF, Pitt MLM. 2015. Ebola virus infections in nonhuman primates are temporally influenced by glycoprotein poly-U editing site populations in the exposure material. Viruses 7:6739–6754. https://doi.org/10.3390/v7122969.
30. Boudko SP, Kuhn RJ, Rossmann MG. 2007. The coiled-coil domain structure of the Sin Nombre virus nucleocapsid protein. J Mol Biol 366:1538–1544. https://doi.org/10.1016/j.jmb.2006.12.046.
31. Wang Y, Boudreaux DM, Estrada DF, Egan CW, St Jeor SC, De Guzman RN. 2008. NMR structure of the N-terminal coiled coil domain of the Andes hantavirus nucleocapsid protein. J Biol Chem 283:28297–28304. https://doi.org/10.1074/jbc.M804869200.
32. Guo Y, Wang W, Sun Y, Ma C, Wang X, Wang X, Liu P, Shen S, Li B, Lin J, Deng F, Wang H, Lou Z. 2016. Crystal structure of the core region of hantavirus nucleocapsid protein reveals the mechanism for ribonucleoprotein complex formation. J Virol 90:1048–1061. https://doi.org/10.1128/JVI.02523-15.
33. Yoshimatsu K, Arikawa J. 2014. Antigenic properties of N protein of hantavirus. Viruses 6:3097–3109. https://doi.org/10.3390/v6083097.
34. Hardcastle K, Scott D, Safronetz D, Brining DL, Ebihara H, Feldmann H, LaCasse RA. 2016. Laguna Negra virus infection causes hantavirus pulmonary syndrome in Turkish hamsters (*Mesocricetus brandti*). Vet Pathol 53:182–189. https://doi.org/10.1177/0300985815570071.
35. Kanerva M, Melén K, Vaheri A, Julkunen I. 1996. Inhibition of Puumala and Tula hantaviruses in Vero cells by MxA protein. Virology 224:55–62. https://doi.org/10.1006/viro.1996.0506.
36. Pavlovic J, Schröder A, Blank A, Pitossi F, Staeheli P. 1993. Mx proteins: GTPases involved in the interferon-induced antiviral state. Ciba Found Symp 176:233–247.
37. Khaiboullina SF, Rizvanov AA, Lombardi VC, Morzunov SP, Reis HJ, Palotás A, St Jeor S. 2013. Andes-virus-induced cytokine storm is partially suppressed by ribavirin. Antivir Ther 18:575–584. https://doi.org/10.3851/IMP2524.
38. Cimica V, Dalrymple NA, Roth E, Nasonov A, Mackow ER. 2014. An innate immunity-regulating virulence determinant is uniquely encoded by the Andes virus nucleocapsid protein. mBio 5:e01088-13. https://doi.org/10.1128/mBio.01088-13.
39. Wang Z, Mir MA. 2015. Andes virus nucleocapsid protein interrupts protein kinase R dimerization to counteract host interference in viral protein synthesis. J Virol 89:1628–1639. https://doi.org/10.1128/JVI.02347-14.
40. Goodbourn S, Didcock L, Randall RE. 2000. Interferons: cell signalling, immune modulation, antiviral response and virus countermeasures. J Gen Virol 81:2341–2364. https://doi.org/10.1099/0022-1317-81-10-2341.
41. Ly HJ, Ikegami T. 2016. Rift Valley fever virus NSs protein functions and the similarity to other bunyavirus NSs proteins. Virol J 13:118. https://doi.org/10.1186/s12985-016-0573-8.
42. von Heijne G. 1999. Recent advances in the understanding of membrane protein assembly and structure. Q Rev Biophys 32:285–307. https://doi.org/10.1017/s0033583500003541.
43. Mittler E, Wec AZ, Tynell J, Guardado-Calvo P, Wigren-Byström J, Polanco LC, O'Brien CM, Slough MM, Abelson DM, Serris A, Sakharkar M, Pehau-Arnaudet G, Bakken RR, Geoghegan JC, Jangra RK, Keller M, Zeitlin L, Vapalahti O, Ulrich RG, Bornholdt ZA, Ahlm C, Rey FA, Dye JM, Bradfute SB, Strandin T,

Downloaded from https://journals.asm.org/journal/msphere on 06 June 2023 by 200.51.93.114.

Herbert AS, Forsell MNE, Walker LM, Chandran K. 2022. Human antibody recognizing a quaternary epitope in the Puumala virus glycoprotein provides broad protection against orthohantaviruses. Sci Transl Med 14:eabl5399. https://doi.org/10.1126/scitranslmed.abl5399.
44. National Research Council. 2011. Guide for the care and use of laboratory animals, 8th ed. National Academies Press, Washington, DC.
45. Padula P, Figueroa R, Navarrete M, Pizarro E, Cadiz R, Bellomo C, Jofre C, Zaror L, Rodriguez E, Murúa R. 2004. Transmission study of Andes hantavirus infection in wild sigmodontine rodents. J Virol 78:11972–11979. https://doi.org/10.1128/JVI.78.21.11972-11979.2004.
46. Bellomo CM, Pires-Marczeski FC, Padula PJ. 2015. Viral load of patients with hantavirus pulmonary syndrome in Argentina. J Med Virol 87:1823–1830. https://doi.org/10.1002/jmv.24260.
47. Alonso DO, Pérez-Sautu U, Bellomo CM, Prieto K, Iglesias A, Coelho R, Periolo N, Domenech I, Talmon G, Hansen R, Palacios G, Martinez VP. 2020. Person-to-person transmission of Andes virus in hantavirus pulmonary syndrome, Argentina, 2014. Emerg Infect Dis 26:756–759. https://doi.org/10.3201/eid2604.190799.
48. Katoh K, Standley DM. 2013. MAFFT multiple sequence alignment software version 7: improvements in performance and usability. Mol Biol Evol 30:772–780. https://doi.org/10.1093/molbev/mst010.
49. Minh BQ, Schmidt HA, Chernomor O, Schrempf D, Woodhams MD, von Haeseler A, Lanfear R. 2020. IQ-TREE 2: new models and efficient methods for phylogenetic inference in the genomic era. Mol Biol Evol 37:1530–1534. https://doi.org/10.1093/molbev/msaa015.
50. Kalyaanamoorthy S, Minh BQ, Wong TKF, von Haeseler A, Jermiin LS. 2017. ModelFinder: fast model selection for accurate phylogenetic estimates. Nat Methods 14:587–589. https://doi.org/10.1038/nmeth.4285.
51. Taylor MK, Williams EP, Wongsurawat T, Jenjaroenpun P, Nookaew I, Jonsson CB. 2020. Amplicon-based, next-generation sequencing approaches to characterize single nucleotide polymorphisms of orthohantavirus species. Front Cell Infect Microbiol 10:565591. https://doi.org/10.3389/fcimb.2020.565591.

Downloaded from https://journals.asm.org/journal/msphere on 06 June 2023 by 200.51.93.114.